Molecular dynamics simulation of the viscocapillary leveling of polymer films

I. Tanis[1], H. Meyer[2], T. Salez[1,3], E. Raphaël[1], A.C. Maggs[1] and J. Baschnagel[2]

[1]Laboratoire de Physico-Chimie Théorique, UMR CNRS Gulliver 7083,
ESPCI Paris, PSL Research University, 75005 Paris, France

[2]Université de Strasbourg, CNRS, Institut Charles Sadron, UPR 22, 67000 Strasbourg, France

[3]Global Station for Soft Matter, Global Institution for Collaborative Research and Education,
Hokkaido University, Sapporo, Hokkaido 060-0808, Japan

Abstract. Surface tension-driven flow techniques have recently emerged as an efficient means of shedding light into the rheology of thin polymer films. Motivated by experimental and theoretical approaches in films bearing a varying surface topography, we present results on the viscocapillary relaxation of a square pattern at the free surface of a polymer film, using molecular dynamics simulations of a coarse-grained polymer model. Height profiles are monitored as a function of time after heating the system above its glass-transition temperature. The associated relaxation rates are in agreement with the low-Reynolds-number hydrodynamic model, thus confirming the utility of the simulation method.

I. Introduction

Thin polymer films have emerged as a class of glass-forming materials with a potential for a wide number of nanoscale applications. Given the appealing properties such as (in general) low thermal conductivity and high dielectric constant, these systems are utilized in a variety of technological fields such as micro-electronics,[1,2] coatings in optical fibers[3] and nanolithography.[4] To this end, their static and dynamic properties and deviations from bulk behaviour due to spatial restriction and interfacial effects have been the subject of extensive research and debate over the last years.[5-8] Particular attention has been focused on the rheological behaviour of thin polymer films as well as on the dynamical heterogeneities triggered by the presence of interfaces.[9-12] A striking feature observed in films with a free interface is the enhanced mobility in a region near the surface, as suggested by recent

reports.[9,13,14] Such behaviour has also been detected in small-molecule glasses.[15-20] An efficient and versatile method to probe the aformentioned attributes is the capillary driven relaxation of an imposed topography on the film surface. In this context, a recent experimental approach addressed the viscocapillary leveling of polystyrene stepped films.[21] After heating well above the glass-transition temperature T_g, the excess surface area was allowed to relax under the effect of the Laplace pressure. By deriving the flow equations based on the lubrication approximation,[22] a measurement of the viscosity of the film was accomplished.[23,24] Furthermore, below T_g the analysis suggests the existence of a thin mobile layer near the surface, whereas at elevated temperature the whole film flows.[25] The experimentally determined height profiles were in excellent agreement with the solution of the capillary-driven thin film equation which was found to converge in time to a self-similar profile.[23,24,26]

Molecular dynamics (MD) simulation has been a valuable tool for the elucidation of the mecanisms that determine the behaviour of polymers in confinement.[6,9,27-34] Given the wide spread of length and time scales that govern the structure and dynamics of such systems, different approaches and certain simplifications have been developed in order to meet the requirements of the system under study. The dramatic increase of the relaxation time upon approaching the glassy state is common to all polymers regardless of the underlying chemistry. This fact allows for the utilization of a simplified model with generic features of the polymer chain. Several studies employing such models have addressed interfacial effects on the glass transition and the alteration of the latter depending on film thickness, confinement-induced changes in polymer conformations and polymer-substrate interactions[35-45] Smooth or rough walls with varying monomer-wall interaction strength have been used as substrates. A complex dynamical behaviour upon approaching the glass transition has been observed whereas shifts from the bulk T_g were found in agreement with experimental measurements.[9,30] However, to the authors' knowledge, there is no simulation work considering polymer films with a stepped surface topography near the glass transition. As capillary leveling has been proved an efficient tool to probe surface mobility, the purpose of this contribution is to examine the evolution of thin supported films with a square surface pattern, using molecular dynamics simulations ; thus complementing the existing experimental and theoretical approaches relying on a global knowledge of the surface profile with a newly accessible inner information at the molecular level. We monitor the evolution of the film and the leveling process at temperatures above T_g. Simulation results are compared with an analytical solution of the Stokes equation assuming a small amplitude of the

perturbation. This allows a linearization of the problem and application of Fourier analysis.[4,24] In section II the simulation model and the preparation of the polymer films are described whereas section III provides the analytical solution of a periodic square profile. Section IV provides a discussion of our results and a comparison of the simulation and analytical approaches. The final section summarizes our findings. An investigation of the polymer-substrate boundary condition as well as the local inner dynamics as a function of the distance from the wall, is presented in the Appendix. This examination considers either smooth, weakly attractive substrates described implicitly by a wall potential or substrates modeled explicitly by incorporating a hexagonal lattice.

II. Simulation protocol

A generic bead-spring (BS) model for a polymer melt which has been successfully utilized in analogous studies of thin polymer films, is used for the molecular dynamics simulations of this work.[29,46] The model assumes linear, flexible chains for which only the connectivity and non-bonded monomer-monomer interactions for all but the nearest neighbors along the chain are taken into account. The connectivity between adjacent monomers of a chain separated by a distance r is assured by a harmonic-spring potential with equilibrium distance $l_b = 0.967\sigma$ and spring constant $k_b = 1111\ \varepsilon/\sigma^2$:

$$U_b = \frac{k_b}{2}(r - l_b)^2, \tag{1}$$

where k_b has been chosen large enough in order that chains cannot cut through each other, thus allowing the formation of entanglements. Non-bonded monomer-monomer interactions are described by a truncated and shifted Lennard-Jones (LJ) potential with cut-off radius, $r_c = 2.3\sigma \simeq 2r_{min}$ where r_{min} is the minimum of the LJ potential:

$$U_{LJ}(r) = 4\varepsilon\left[\left(\frac{\sigma}{r}\right)^{12} - \left(\frac{\sigma}{r}\right)^{6}\right] - U_{LJ}(r_c), \quad r \le r_c\,. \tag{2}$$

This BS model is very similar to other models recently used in simulation studies of polymers in confinement.[27,31,39]

All simulation results are given in LJ units. The LJ parameters of the monomers as well as their mass are set to unity. Length is measured in σ, energy in ε, temperature in unit of ε/k_B ($k_B = 1$), time in unit of $\tau_{LJ} = \sqrt{m\sigma^2/\varepsilon}$, viscosity in unit of $\tau_{LJ}\varepsilon/\sigma^3$ and surface tension in ε/σ^2. The model exhibits two intrinsic length scales, corresponding to the minima of the

bond and LJ potentials. The existence of these distinct lengths in conjunction with the chain flexibility would allow us to assume that the system remains amorphous at low temperatures as shown in several works.[31,43,44] Nevertheless, recent studies report that bead-spring models widely used in systems in confinement, are subjected to heterogenous nucleation when exposed to explicit crystalline substrates.[47] We should note here that no signs of crystallization were detected in our study. The polymer sample consists of a total number of n = 8064 chains, each bearing a number of monomers of N = 16. This chain length is below the estimated entanglement length, found to be $N_c \simeq 32$ [48,49] or $N_c \simeq 64$ based on primitive path analysis.[50]

We examine systems of supported films with one polymer-substrate and one free (polymer-vaccum) interface. Two types of substrates were considered and described in detail in the Appendix. At the first stage, a smooth, weakly attractive structureless wall was introduced to model the polymer-substrate interaction. As shown in the Appendix, this representation imparts a slip boundary condition and layering extending over several monomer diameters. On the other hand, the incorporation of explicit substrate particles with perturbed coordinates with respect to a periodic lattice, was found to inhibit polymer slippage and restrict density modulation to a few monomer diameters. The latter case constitutes an adequate representation of the established boundary condition for polystyrene on a silicon substrate in the experimental approaches.[21,23-26] Consequently, all films described below are supported on explicit substrate particles.

All simulations were conducted via the LAMMPS[51] code in the canonical (NVT) ensemble. As conservation of momentum is important for the system under study, temperature was maintained through the use of the Dissipative Particle Dynamics (DPD) thermostat (pair friction)[52] which controls temperature via the balance of a random force that injects energy into the system and a friction force dissipating energy. For that thermostat, a coupling constant ζ = 1 and a cutoff function $w(r_{ij}) = 1 - \frac{r_{ij}}{r_c}$, were used, with r_{ij} being the distance between a pair of monomers and the cutoff being the same as that of the LJ potential.[52] The equations of motion were integrated by the Velocity Verlet algorithm with a time step of 0.005. Periodic boundary conditions were applied in the parallel xz directions. In a previous work, the glass transition temperature of supported and free-standing polymer films was estimated by monitoring the film thickness upon cooling.[46,53] The authors reported a minor reduction of the T_g ($T_g \approx 0.38$) for supported films of chain length N = 10 with respect to corresponding samples in the bulk ($T_g \approx 0.39$). Furthermore, for the purpose of the present

study, additional runs performed on free-standing films of thicknesses D = 5,10,20 showed that for $D \geq 10$, mechanical stability was maintained for temperatures up to T = 1 and no "evaporation" of chains was observed.

In order to perform a comparison of the simulation with the hydrodynamic model, an estimation of the dynamic viscosity and surface tension is required. The former property was calculated in the bulk state whereas flat films of thickness $D \approx 20$ were prepared for the surface tension calculations. The shear viscosity η, can be extracted from the Green-Kubo formula, i.e. by integrating over time the autocorrelation function of the stress tensor[54] as:

$$\eta = \frac{V}{k_B T} \int_0^\infty \langle P_{ij}(t) P_{ij}(0) \rangle dt \,, \tag{3}$$

where V stands for the volume of the system, T is the temperature, k_B is the Boltzmann constant, P_{ij} refers to the shear component of the stress tensor, the angle bracket denotes the ensemble average and t is time. An alternative way to determine the shear viscosity is via the implementation of the Mueller-Plathe algorithm.[55] Both methods were tested at T = 0.5 and yielded similar results. The surface tension was estimated via the local (per atom) stress tensor. Each component can be extracted by counting the number of monomers in a layer at height y, calculating the pressure in the layer and afterwards averaging over all monomers in the layer.[56] Integration of the difference between the normal ($P_\perp$) and tangential ($P_\parallel$) components yields the surface tension γ as:[53]

$$\gamma = \int_{D/2}^{\infty} [P_\perp(y) - P_\parallel(y)] \mathrm{d}y \tag{4}$$

where y is the direction perpendicular to the film interface and D / 2 the center of the film. Our calculations yield $P_\perp \approx 0$ for all y as required by mechanical stability. Table 1 lists the shear viscosity and surface tension data calculated at T = 0.44 and 0.5 together with the longest Rouse mode chain relaxation times, τ_R. The relation between η and τ_R at the target temperatures T_1 = 0.44 and T_2 = 0.50 was examined and found to be in good agreement with the expectation from the Rouse model:

$$\frac{\eta_1}{\eta_2} \approx \frac{\tau_{R1} \rho_1 T_1}{\tau_{R2} \rho_2 T_2} \,, \tag{5}$$

where we have used the approximations $\rho_1 T_1 \approx 0.45$ and $\rho_2 T_2 \approx 0.50$. [57]

Table 1: Dynamic viscosity, surface tension and relaxation times of the polymer chains at T = 0.44 and 0.50. Error bars are $\pm$5% for the viscosity and $\pm$1% for the surface tension.

T	η	γ	τ_R
0.44	3000	1.58	100765
0.50	300	1.44	10980

At the first stage of the patterned-film preparation, we introduced structureless walls at y = 0 and $y = B_y$ via eq.A1 to a well relaxed piece of film of thickness $D \approx 15$ and of n = 1152 chains (box dimensions: B_x = 52.4832 and $B_y = B_z$ = 26.2416) at a very low temperature of T = 0.1. This initial configuration was heated to T = 0.50. To do so, temperature was continuously increased at a rate of 2×10^{-4}. After completion of the heating process, the obtained configuration was used as a starting point for an isothermal run at T = 0.5. The length of this run was sufficiently long in order to achieve a relaxation of the auto-correlation function of the chain end-to-end vector. The equilibrated configuration was used as base unit for the construction of the patterned film at T = 0.1. Two layers of substrate particles were inserted slightly above the structureless impenetrable wall. The piece of film was afterwards replicated in the x-direction and shifted in the y-direction to create the bottom polymer layer. An additional insertion and shift of the base unit in both x and y directions was performed in order to obtain the desired surface topography. This procedure finally yields a periodic square pattern with a vertical aspect ratio of 1:3. The resulting topography is invariant in the z direction. Similarly to the procedure described earlier, the patterned film was heated up to T = 0.44 and 0.50. The configuration obtained after heating was used as the starting point for the isothermal runs and is illustrated in fig.1. It should be noted here that, for a number of the prepared systems, additional relaxation steps were performed to the bottom polymer layer (highlighted in blue in fig.1) to assure the adhesion of the layers and allow for some mixture of the chains. This pre-equilibration stage was found to have a minor effect on the leveling process.

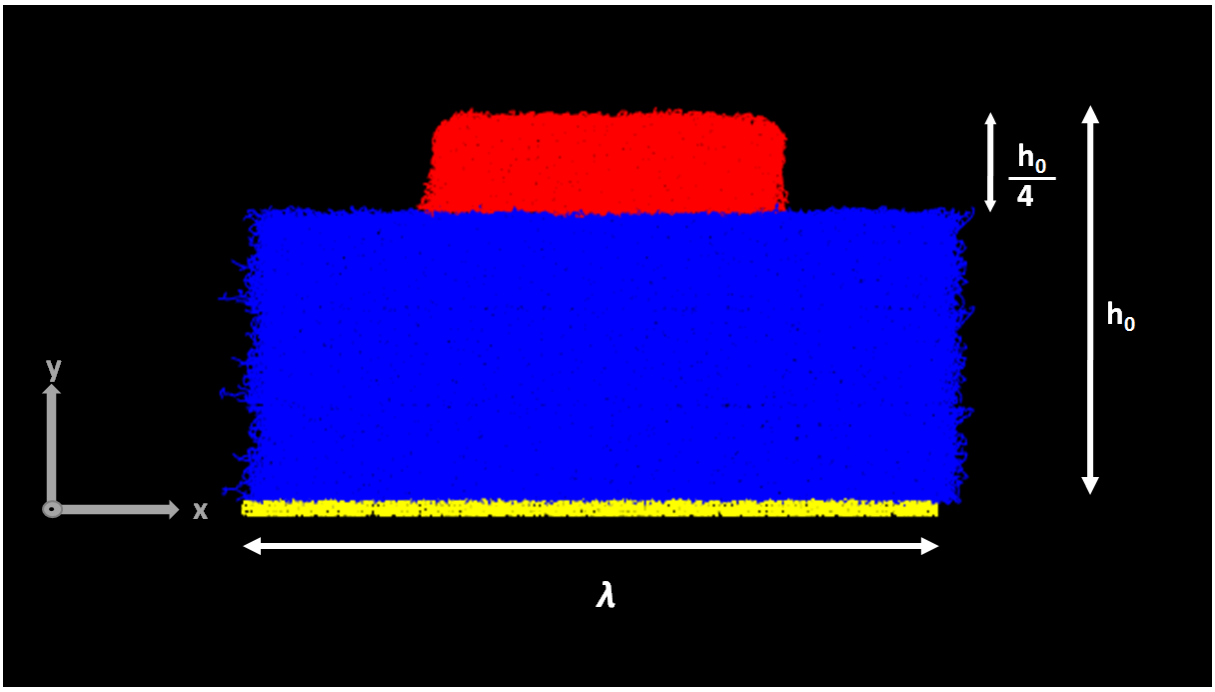

Figure 1 : Configuration of the polymer film model bearing a total number of n = 8064 chains of N = 16 monomers each, after the heating stage to T = 0.44. Periodic boundary conditions are applied in the horizontal x, z directions. λ stands for the horizontal wavelength, i.e. the x-dimension of the simulation box, $2B_x$ and h_0 = 55.9 is the maximum vertical height (color code : red = top layer, blue = bottom layer, yellow = substrate).

III. Theory

In order to characterize the profile evolution obtained from the MD simulations, we invoke the following hydrodynamic model. We consider a thin viscous film of constant dynamic viscosity η and surface tension γ with the ambient atmosphere. At t = 0, the initial film profile is a periodic symmetric square pattern with the same vertical aspect ratio as the one depicted in fig.1, the maximum vertical height (counted from the substrate) of which is noted $h(0) = h_0$ and the horizontal wavelength noted λ. At finite time t, the maximum height is noted $h(t)$. Due to the chosen aspect ratio and invoking conservation of volume, the long-time fully-leveled flat state is characterized by a uniform height with limit $h_\infty = \lim_{t\to+\infty} h(t) = 7h_0/8$. By invoking low-Reynolds-number hydrodynamics with a no-slip boundary condition at the substrate and a no-shear boundary condition at the free interface and assuming that the surface perturbation is small, it is possible to show[4,58] that each Fourier mode of the profile with nonzero wave vector k decays exponentially with a rate determined by k, h_∞, γ and η. Focusing only on the dominant mode $k = 2\pi/\lambda$ of the problem, we explicitly have :

$$\ln\left[\frac{h(t)-h_\infty}{h_0-h_\infty}\right] = -\left[\frac{\gamma k}{2\eta}\frac{e^{2kh_\infty}-e^{-2kh_\infty}-4kh_\infty}{e^{2kh_\infty}+2+e^{-2kh_\infty}+4(kh_\infty)^2}\right]t\,, \qquad (6)$$

which is the law of interest to be compared to the molecular dynamics leveling results and defines the relaxation rate for arbitrary confinement.[4] To verify that our simulation method satisfies the assumptions of the hydrodynamic model, we evaluated the Reynolds number at the two target temperatures using the formula $\mathrm{Re} = \rho h_0 u_c/\eta$, where ρ is the monomer density, η the viscosity, h_0 the vertical maximum height and $u_c = \gamma/\eta$ the capillary velocity. Substitution of the numerical values yields a Reynolds number of the order of 10^{-5} at T = 0.44 and of the order of 10^{-3} at T = 0.50 respectively, thus indicating the viscous nature of the simulated flow. In addition, the stress tensor calculations described in Section II yield a zero value for the shear stress at the free surface, also in agreement with theory.

IV. Results

As stated in Section II, the configuration obtained after the heating of the patterned film was used as the starting point for the isothermal runs. The duration of the run was long enough to assure substantial leveling. The temporal evolution of the profile at both temperatures is illustrated in fig.2.

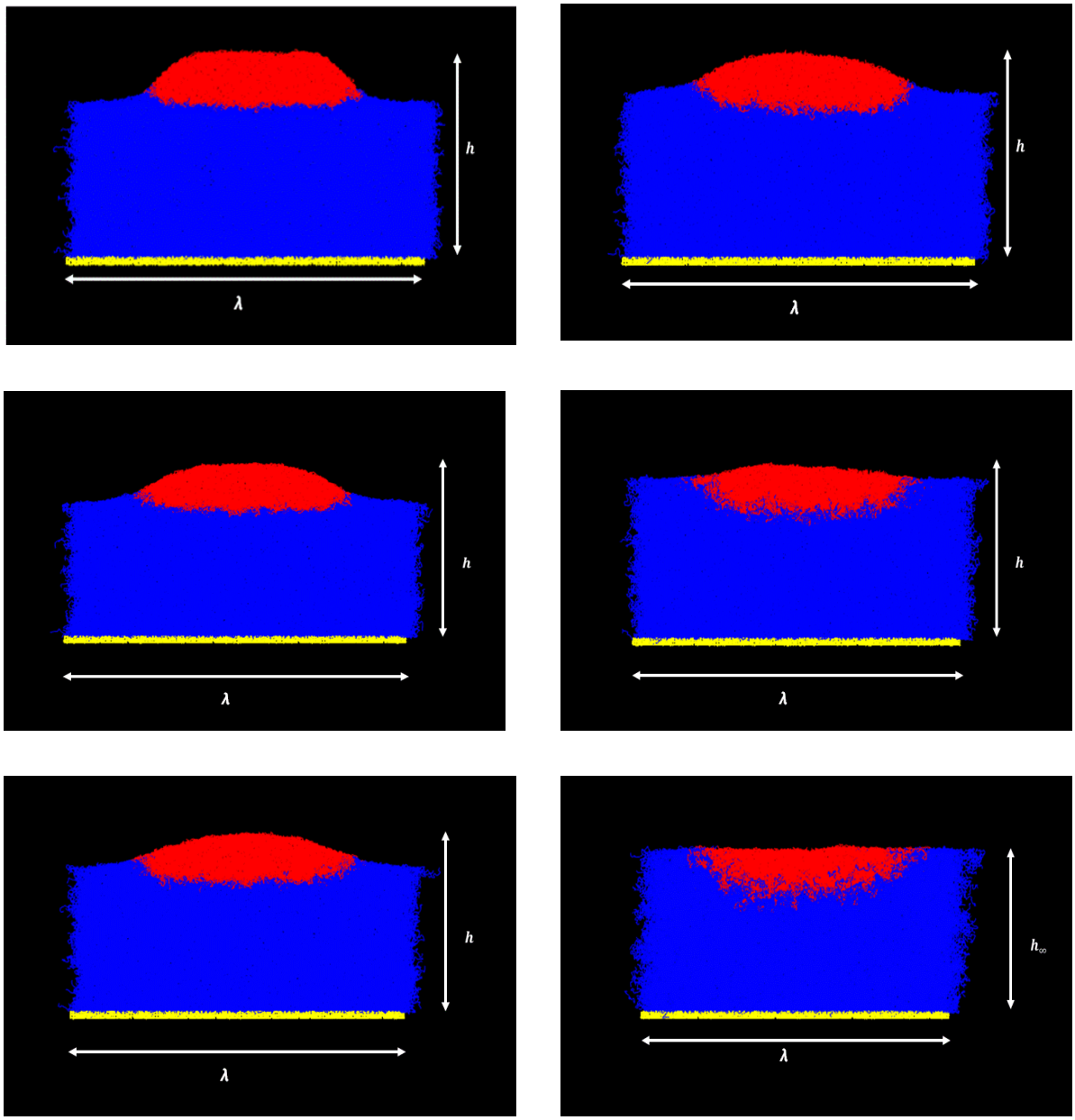

Figure 2: Time evolution of the square pattern (see fig.1) at T = 0.44 (left panels) and T = 0.50 (right panels). From top to bottom: $t/10^3$ = 5, 20, 45. Note that at the bottom right panel full leveling has been accomplished ($h = h_\infty$). The expected decay times for unconfined relaxation defined as $\tau^* = 2\,\eta/(\gamma k)$, are $\tau^* = 63468$ for T = 0.44 and $\tau^* = 6963$ for T = 0.50 respectively.

A clear difference in the film evolution is observed at the two different temperatures. This is anticipated as at T = 0.44 the film is still close enough to its T_g and chain motion remains restricted whereas at T = 0.50 the system adopts the behaviour of a liquid. As can be seen from the right panels, complete leveling is reached at T = 0.50 in a time scale of the order of 50×10^3. On the other hand, at T = 0.44 leveling is only partial and complete leveling (not shown) is seen at about 330×10^3. To gain quantitative insight on the leveling process, we have

monitored the corresponding height profiles h(x,t). The latter are provided in fig.3.

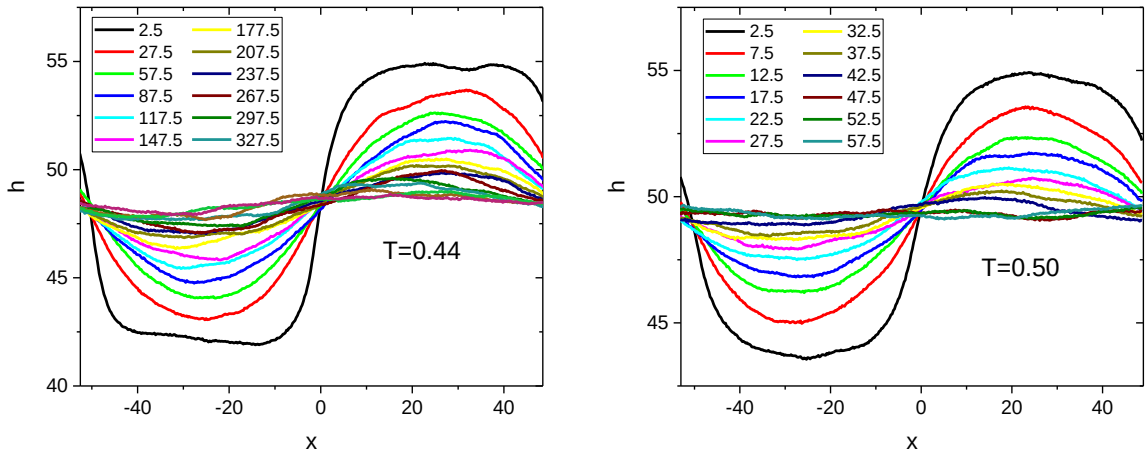

Figure 3: Height profiles of the square film (figs.1 and 2) during the time evolution at T = 0.44 (left) and T = 0.50 (right). The different times (t/10^3) are indicated in the legend whereas x = 0 corresponds to the position of the left side of the step.

A visual inspection of the obtained profiles reveals an absence of "bumps" and "dips" on the respective thick and thin sides of the film in contrast to experimental findings in stepped polystyrene films.[21] Moreover, an examination of the profiles at early times has not shown any clear indication of self-similar behaviour contrary to the aforementioned case.[23] This is due to the fact that these previous studies were performed in the domain of validity of the lubrication approximation (for which the typical horizontal length scale is much larger than the vertical one) and that their initial patterns were not periodic. This approximation and symmetry assumes $kh_\infty \ll 1$ contrary to our case where $kh_\infty \approx 3$. Analogous findings are reported in a combined experimental and analytical study targeted for nanoimprint lithography.[4] On these grounds, eq.6 is more general and valid for our thick system.

To perform a direct comparison with the hydrodynamic model described in Section III, we plot the relative amplitude, $\ln\left[\frac{h(t)-h_\infty}{h_0-h_\infty}\right]$, as a function of time t, where h_0 is the maximum height of the configuration obtained after the completion of the heating process (t = 0), h_∞ is the final height of the fully leveled film and h(t) is the maximum height value of each isothermal run at time t. The presented data for T = 0.44 constitute averages over the profiles of two independent samples whereas at T = 0.50 seven independent samples were used. The corresponding graphs for both examined temperatures are displayed in fig.4.

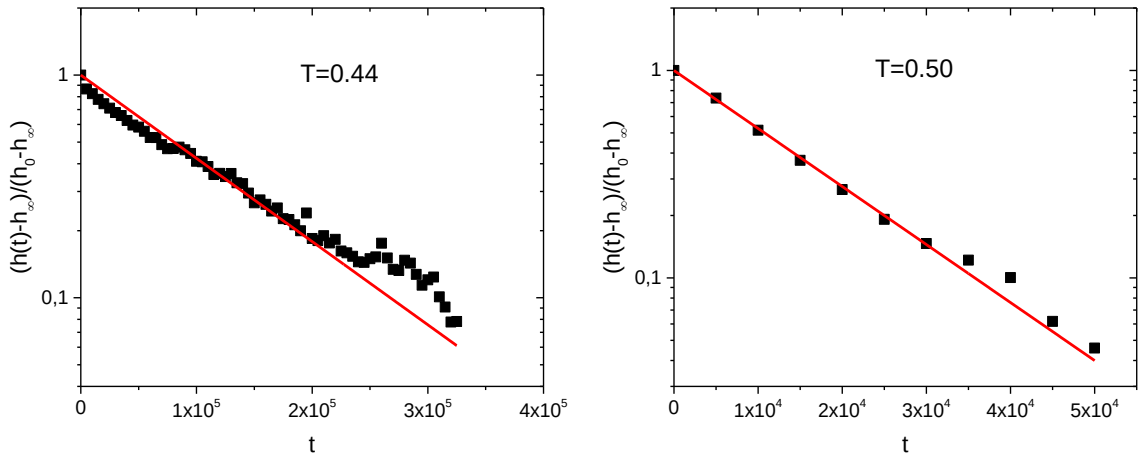

Figure 4: Time evolution of the relative amplitude at T = 0.44 (left) and T = 0.50 (right). The red lines passing through the data are linear fits.

As it can be seen, the relative amplitude decays exponentially in accordance with the hydrodynamic model of Section III. The fits to the data yield a rate of $8.60 \times 10^{-6} \pm 1.72 \times 10^{-7}$ at T = 0.44 whereas at T = 0.50 the corresponding rate is $6.44 \times 10^{-5} \pm 9.07 \times 10^{-7}$. Substitution of the h_∞, h_0, k, γ and η values for our system in the hydrodynamic model yields rates of 1.38×10^{-5} and 1.27×10^{-4} for T = 0.44 and T = 0.50, respectively. Simulated rates appear similar but slower as compared to their analytical counterparts, with the difference reaching a factor of about 2 at T = 0.50 whereas a better agreement is reported at the lower temperature studied. Since the rate is inversely proportional to the viscosity, this difference would imply that the viscosity of the film is about a factor of 2 larger than in the bulk, in contrast to expectation for other studies of the film dynamics, e.g.[46] However, the discrepancy between the theoretical and modeling approaches may also be attributed to the fact that the theoretical solution assumes a vanishingly small profile perturbation with respect to the flat configuration. A vertical aspect ratio of 1:3 chosen in this study as a reasonable compromise between the theoretical requirements and the demands in computational power, is only an approximation to this assumption. Moreover, it should be noted that the theoretical approach assumes the viscosity to remain constant throughout the film. Neither possible short-time effects nor modified surface mobility are taken into account, which might however affect the MD results. Nevertheless, in the absence of any fitting parameter, the obtained close similarity between the time scales from MD and hydrodynamic approaches is encouraging, inviting a more detailed comparison between the MD simulation and the theory of capillary leveling processes, also at temperature below *T*g.

IV. Conclusions

Molecular dynamics simulations have been conducted in order to examine the relaxation of a thin polymer film the surface of which bears a periodic square pattern. A generic bead-spring model was utilized to model the polymer chains. Concurrently, the full Stokes film equation was linearised (assuming a stepped perturbation in the initial profile) allowing thus for an analytical solution. The evolution of the height profiles was analyzed after heating above the glass-transition temperature. The relaxation rates in the liquid state were found to be faster by a factor of about 8 as compared to the respective rates, in the vicinity of the glass-transition temperature. Simulation results are in approximate agreement with hydrodynamic predictions, indicating the robustness of our novel molecular dynamics modeling of the capillary leveling of thin polymer films. Therefore, this work opens the way to the study of viscocapillary effects in complex fluids and polymer glasses via molecular dynamics simulation.

Acknowledgements

The authors gratefully acknowledge financial support from ANR WAFPI and ANR FSCF, as well as the Global Station for Soft Matter, a project of Global Institution for Collaborative Research and Education at Hokkaido University. They thank Kari Dalnoki-Veress, James Forrest, Joshua McGraw, and Oliver Bäumchen for stimulating discussions and experimental insights.

Appendix. Hydrodynamic boundary condition: Control and characterization

As expected in a supported polymer film, the established hydrodynamic boundary condition is governed by the interaction of the polymer liquid with the substrate, together with the structure of the latter. Simulation tests were performed on a flat film of thickness $D \approx 20$. At an initial stage, we implicitly introduced a wall at $y = 0$ in the xz-plane of the simulation box. The monomer-wall interaction was modeled by a nontruncated 9-3 LJ-potential

$$U_{\mathrm{w}}(y) = \varepsilon_{\mathrm{w}} \left[\left(\frac{\sigma}{y}\right)^9 - \left(\frac{\sigma}{y}\right)^3 \right], \qquad \text{(A.1)}$$

where y stands for the distance from the wall and ε_{w} for the potential depth. This formula can be obtained by integrating the LJ interactions between the wall atoms and monomers. To examine the effect of explicit substrate particles on the boundary condition, an additional model was generated. Two layers of substrate particles were inserted above the structureless

wall. These substrate particles were generated as a crystalline lattice, the positions of which were randomly displaced by up to 25% of a lattice spacing. The size of the particles was chosen to be the same as the monomer size, whereas the monomer-substrate interaction strength was chosen to be the same as that between the monomers. This choice of LJ parameters in conjunction to a monomer density $\rho \sim 1$, has been shown to enhance the ability of the polymer chains to adapt to the wall structure, thus leading to a "stick boundary condition".[6,59,60] The substrate particles were fixed to their positions by stiff springs of constant $k_s = 200\ \varepsilon/\sigma^2$. Both systems were generated at $T = 0.1$ and heated to $T = 0.5$ at a rate equal to the one stated in Section II. Isothermal runs of 800000 steps were launched after reaching the target temperature. Figure A1 displays the monomer density profiles of the examined systems at $T = 0.5$.

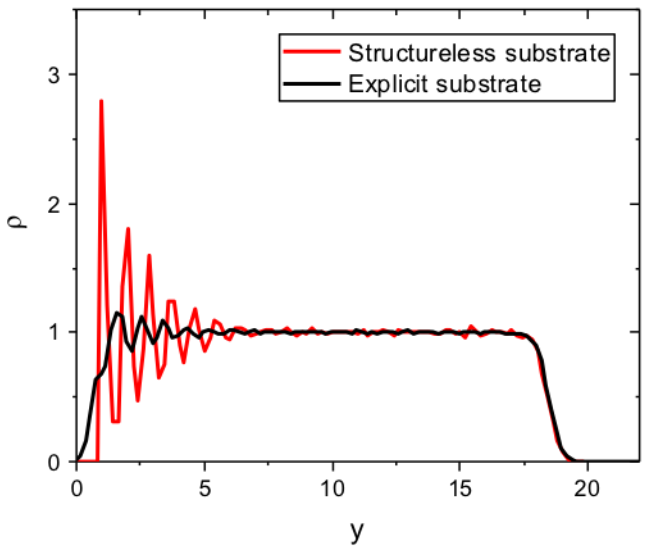

Figure A1: Monomer density profiles for a film supported on a wall represented either implicitly or by explicit substrate particles. The profile of the system corresponding to the latter case has been shifted in the *x*-axis in order that the positions of the free surface of both systems coincide.

Figure A2 presents the layer-resolved incoherent intermediate scattering function calculated at $q = 6.9$, the position of the maximum of the static structure factor :

$$\varphi_q^{s\parallel}(t,y) = \left\langle \frac{1}{n_t} \sum_i \prod_{t'=0}^{t} \delta[y - y_i(t')]\, e^{-i\vec{q}\left[\vec{r}_i^{\parallel}(t) - \vec{r}_i^{\parallel}(0)\right]} \right\rangle. \qquad \text{(A. 2)}$$

Here $\vec{r}_i^{\parallel}(t)$ is the position, parallel to the wall, of monomer i at time t and $\varphi_q^{s\parallel}$ is averaged over all film monomers. This definition takes into account only the n_t monomers which are at all times $t < t'$ within the slab centered at y and bearing a width of $\Delta y = 2$. We consider the dynamics in the unconstrained directions x and z.

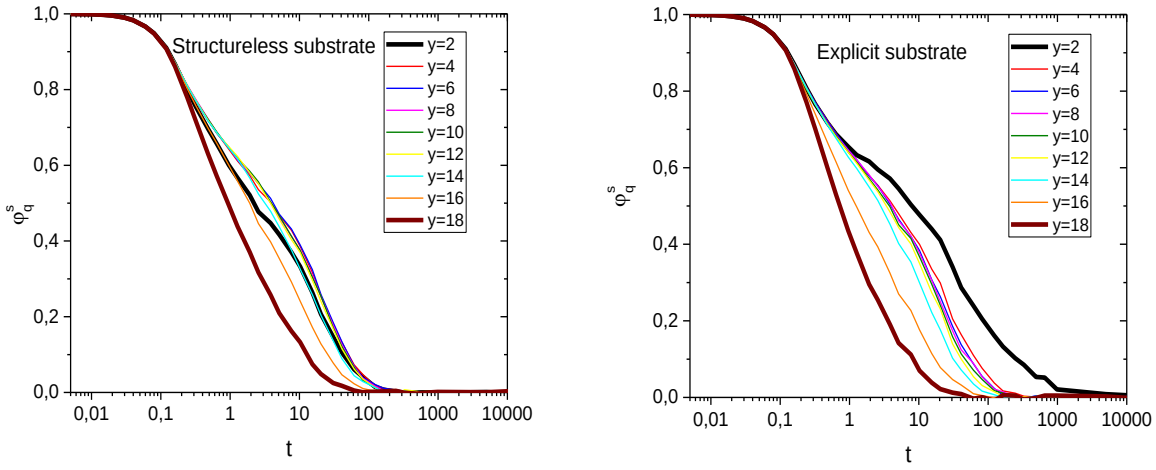

Figure A2: Layer-resolved incoherent scattering function at q = 6.9 (corresponding to the maximum of S(q)) with y being the distance from the substrate at T = 0.5 near a wall represented either implicitly (left) or by explicit substrate particles (right).

As it can be seen in fig.A1, the implementation of explicit substrate particles results in a restriction of density modulations to few monomer diameters, together with a notable reduction of the amplitude of the modulations. Moreover, fig.A2 reveals that the relaxation times increase as we move from the wall to the center of the film and decrease again as we approach the free surface.[46] In contrast, in the explicit case dynamics gets slower upon approaching the wall, thus indicative of a no-slip boundary condition. This dynamical behaviour is in agreement with analogous simulation studies in confined liquids.[6,27,61]

We further proceeded to the examination of the height profiles of films with a square surface pattern supported on both substrates. For reasons of computational efficiency, we considered a system with a 1:1 aspect ratio as illustrated in fig.A3.

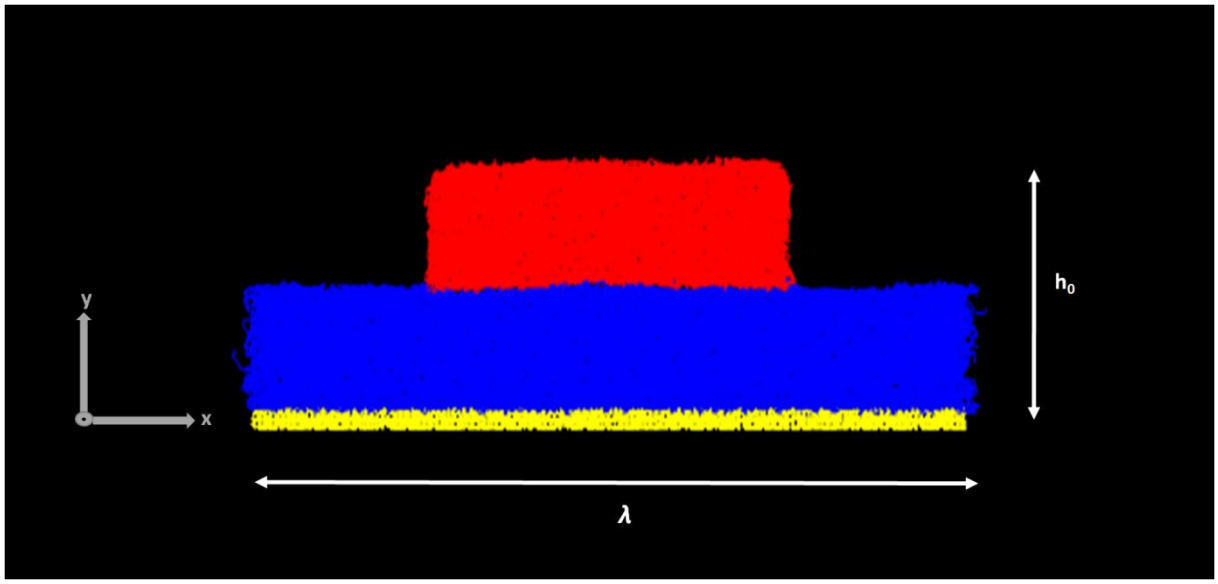

Figure A3 : Polymer film with a square surface profile (periodic boundary conditions in the horizontal directions) placed on an explicit substrate bearing a total number of n = 3456 chains of N = 16 monomers each, after the heating stage to T = 0.44. (color code : red = top layer, blue = bottom layer, yellow = substrate).

The films were prepared and heated to T = 0.44 in a manner analogous to the procedure stated in the main text. The corresponding height profiles are shown in fig.A4.

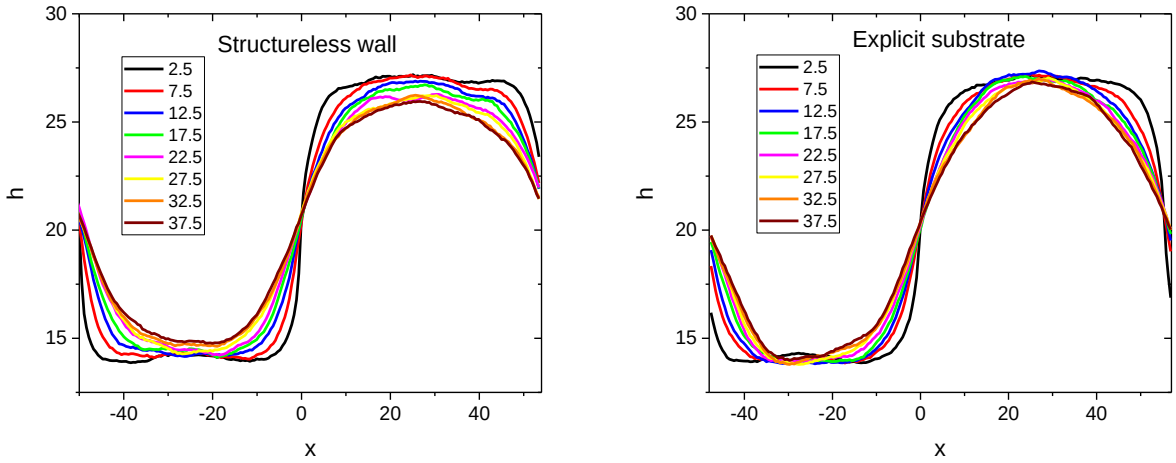

Figure A4 : Height profiles at successive times ($t/10^3$ as indicated in legend) for structureless (left) and explicit (right) substrates. Similarly to fig.3, x = 0 corresponds to the position of the left side of the step.

A different behaviour is observed in the height profiles, where the accelerated dynamics owing to the presence of the weakly attractive smooth wall results in a significantly quicker leveling.

References

[1] J. Ouyang, C.-W. Chu, C. R. Szmanda, L. Ma, and Y. Yang, Nat Mater **3**, 918 (2004).

[2] X. Zhang, and J. P. Bell, Polym. Eng. Sci. **39**, 119 (1999).

[3] J. Rayss, W. M. Podkoś Cielny, and J. Widomski, J. Appl. Polym. Sci. **49**, 835 (1993).

[4] J. Teisseire, A. Revaux, M. Foresti, and E. Barthel, Appl. Phys. Lett. **98**, 013106 (2011).

[5] P. Baglioni, Angew. Chem. Int. Edit. **45**, 1501 (2006).

[6] J. Baschnagel, and F. Varnik, J. Phys.- Condens. Mat. **17**, R851 (2005).

[7] M. D. Ediger, and P. Harrowell, J. Chem. Phys. **137**, 080901 (2012).

[8] A. Mataz, and B. M. Gregory, J. Phys.- Condens. Mat. **17**, R461 (2005).

[9] J.-L. Barrat, J. Baschnagel, and A. Lyulin, Soft Matter **6**, 3430 (2010).

[10] J. A. Forrest, and K. Dalnoki-Veress, Adv. Colloid Interface Sci. **94**, 167 (2001).

[11] T. Leveder, S. Landis, and L. Davoust, Appl. Phys. Lett. **92**, 013107 (2008).

[12] E. Rognin, S. Landis, and L. Davoust, Phys. Rev. E **84**, 041805 (2011).

[13] Z. Fakhraai, and J. A. Forrest, Science **319**, 600 (2008).

[14] Z. Yang, A. Clough, C.-H. Lam, and O. K. C. Tsui, Macromolecules **44**, 8294 (2011).

[15] C. W. Brian, and L. Yu, J. Phys. Chem. A **117**, 13303 (2013).

[16] C. W. Brian, L. Zhu, and L. Yu, J. Chem. Phys. **140**, 054509 (2014).

[17] R. Malshe, M. D. Ediger, L. Yu, and J. J. de Pablo, J. Chem. Phys. **134**, 194704 (2011).

[18] J. H. Mangalara, M. D. Marvin, and D. S. Simmons, J. Phys. Chem. B **120**, 4861 (2016).

[19] W. Zhang, C. W. Brian, and L. Yu, J. Phys. Chem. B **119**, 5071 (2015).

[20] W. Zhang, and L. Yu, Macromolecules **49**, 731 (2016).

[21] J. D. McGraw, N. M. Jago, and K. Dalnoki-Veress, Soft Matter **7**, 7832 (2011).

[22] R. L. Panton, in *Incompressible Flow* (John Wiley & Sons, Inc., 2013), pp. 650.

[23] J. D. McGraw, T. Salez, O. Bäumchen, E. Raphaël, and K. Dalnoki-Veress, Phys. Rev. Lett. **109**, 128303 (2012).

[24] T. Salez, J. D. McGraw, O. Bäumchen, K. Dalnoki-Veress, and E. Raphaël, Phys. Fluids **24**, 102111 (2012).

[25] Y. Chai, T. Salez, J. D. McGraw, M. Benzaquen, K. Dalnoki-Veress, E. Raphaël, and J. A. Forrest, Science **343**, 994 (2014).

[26] T. Salez, J. D. McGraw, S. L. Cormier, O. Bäumchen, K. Dalnoki-Veress, and E. Raphaël, Eur. Phys. J. E **35**, 1 (2012).

[27] P. Z. Hanakata, J. F. Douglas, and F. W. Starr, Nat. Commun. **5**, 4163 (2014).

[28] V. A. Ivanov, A. S. Rodionova, J. A. Martemyanova, M. R. Stukan, M. Müller, W. Paul, and K. Binder, Macromolecules **47**, 1206 (2014).

[29] C.-H. Lam, and O. K. C. Tsui, Phys. Rev. E **88**, 042604 (2013).

[30] C. Mischler, J. Baschnagel, and K. Binder, Adv. Colloid Interface Sci. **94**, 197 (2001).

[31] A. Shavit, and R. A. Riggleman, J. Phys. Chem. B **118**, 9096 (2014).

[32] D. S. Simmons, Macromol. Chem. Physic. **217**, 137 (2016).

[33] M. Solar, and W. Paul, Eur. Phys. J. E **38**, 37 (2015).

[34] W.-S. Tung, R. J. Composto, R. A. Riggleman, and K. I. Winey, Macromolecules **48**, 2324 (2015).

[35] C. Batistakis, and A. V. Lyulin, Comput. Phys. Commun. **185**, 1223 (2014).

[36] T. Davris, and A. V. Lyulin, Polym. Composit. **36**, 1012 (2015).

[37] R. J. Lang, W. L. Merling, and D. S. Simmons, ACS Macro Lett. **3**, 758 (2014).

[38] R. J. Lang, and D. S. Simmons, Macromolecules **46**, 9818 (2013).

[39] W. L. Merling, J. B. Mileski, J. F. Douglas, and D. S. Simmons, Macromolecules **49**, 7597 (2016).

[40] H. Morita, K. Tanaka, T. Kajiyama, T. Nishi, and M. Doi, Macromolecules **39**, 6233 (2006).

[41] J. A. Torres, P. F. Nealey, and J. J. de Pablo, Phys. Rev. Lett. **85**, 3221 (2000).

[42] F. Varnik, J. Baschnagel, and K. Binder, J. Phys. IV France **10**, Pr7 (2000).

[43] F. Varnik, J. Baschnagel, and K. Binder, Phys. Rev. E **65**, 021507 (2002).

[44] F. Varnik, J. Baschnagel, and K. Binder, Eur. Phys. J. E **8**, 175 (2002).

[45] F. Varnik, J. Baschnagel, and K. Binder, J. Non-Cryst. Solids **307–310**, 524 (2002).

[46] S. Peter, H. Meyer, and J. Baschnagel, J. Polym. Sci. Pol. Phys. **44**, 2951 (2006).

[47] M. E. Mackura, and D. S. Simmons, J. Polym. Sci. Pol. Phys. **52**, 134 (2014).

[48] K. Kremer, and G. S. Grest, J. Chem. Phys. **92**, 5057 (1990).

[49] M. Pütz, K. Kremer, and G. S. Grest, EPL-Europhys. Lett. **49**, 735 (2000).

[50] R. Everaers, S. K. Sukumaran, G. S. Grest, C. Svaneborg, A. Sivasubramanian, and K. Kremer, Science 303, 823 (2004).

[51] S. Plimpton, J. Comput. Phys. **117**, 1 (1995).

[52] T. Soddemann, B. Dünweg, and K. Kremer, Phys. Rev. E **68**, 046702 (2003).

[53] S. Peter, Ph.D. thesis, Institut Charles Sadron, Université de Strasbourg, Strasbourg, 2007.

[54] Y. Zhang, A. Otani, and E. J. Maginn, J. Chem. Theory Comput. **11**, 3537 (2015).

[55] F. Müller-Plathe, Phys. Rev. E **59**, 4894 (1999).

[56] S. Plimpton, *LAMMPS: User's Manual* (Sandia National Lab, Albuquerque, 2005).

[57] S. Frey, F. Weysser, H. Meyer, J. Farago, M. Fuchs, and J. Baschnagel, Eur. Phys. J. E 38, 11 (2015).

[58] R. Huang, and Z. Suo, Int.l J. Solids Struct. **39**, 1791 (2002).

[59] J.-L. Barrat, and L. Bocquet, Faraday Discuss. **112**, 119 (1999).

[60] P. A. Thompson, and M. O. Robbins, Phys. Rev. A **41**, 6830 (1990).

[61] P. Scheidler, W. Kob, and K. Binder, EPL-Europhys. Lett. **59**, 701 (2002).